

Consolidation of Al₂O₃ Nano-powder by Magnetic Pulsed Compaction and Sintering

Whung Whoe Kim

Dept. of Nuclear Materials Technology Development, Korea Atomic Energy Research Institute, 150

Dukjin-dong Yuseong-gu Daejeon, 305-353, Korea

1. INTRODUCTION

Nano-alumina powder produced by oxidation and hydrolysis of pure aluminum material [1] is one of the important new ceramic fine materials. One of the critical factors in advanced ceramic technology is synthesis and consolidation of the starting powder. Especially, the consolidation of powder plays an important role in determining the property of a finished component.

The nano-powder that have to be consolidated at high temperature exposure could cause the nanograins to growth resulting in the loss of the superior properties. Unfortunately, however, processing these nanopowders into fully dense, bulk products that retain the original nanoscale grain size has proven to be difficult, owing to a unique combination of problems [2] such as high surface area, severe interparticle friction, and high level of chemisorbed gases. To avoid some of the limitations imposed by exaggerated grain growth and related problems, a number of other consolidation method have been evaluated, such as hot pressing [3], sintering with microwave radiation [4, 5], etc. However, none of these methods have been very successfully in producing fully dense bulk products that retain nanoscale grain size.

Therefore, the consolidation of nanopowder without grain growth is scientifically and technologically important. The most important aspect in the compaction of nanopowders is hot to achieve full density while simultaneously retaining a nanoscale microstructure. Therefore, the process to compact the nanopowder while conserving the nanostructure is strongly required. In our previous work, we proposed to use magnetic pulsed compaction (MPC) for effective consolidation of nano-powder [6-7]. The known data for pressing nano-sized powders by high pulsed pressure give us an opportunity of getting extremely dense compacts with nanostructure and high mechanical properties.

Many researchers have discussed several times throughout the research the difficulty of compacting nano-size powders into green bodies that can be easily examined without crumbling. Nanosize α -Al₂O₃ powder is also very difficult to compact, and high pressures are typically required to obtain structurally sound green bodies. The aim of this research is to consolidate

Report Documentation Page

Form Approved
OMB No. 0704-0188

Public reporting burden for the collection of information is estimated to average 1 hour per response, including the time for reviewing instructions, searching existing data sources, gathering and maintaining the data needed, and completing and reviewing the collection of information. Send comments regarding this burden estimate or any other aspect of this collection of information, including suggestions for reducing this burden, to Washington Headquarters Services, Directorate for Information Operations and Reports, 1215 Jefferson Davis Highway, Suite 1204, Arlington VA 22202-4302. Respondents should be aware that notwithstanding any other provision of law, no person shall be subject to a penalty for failing to comply with a collection of information if it does not display a currently valid OMB control number.

1. REPORT DATE 16 OCT 2007		2. REPORT TYPE FInal		3. DATES COVERED 21-06-2004 to 11-10-2005	
4. TITLE AND SUBTITLE Nano Ceramic materials for High Power Micro-Wave Window				5a. CONTRACT NUMBER FA520904P0407	
				5b. GRANT NUMBER	
				5c. PROGRAM ELEMENT NUMBER	
6. AUTHOR(S) Whung Whoe Kim				5d. PROJECT NUMBER	
				5e. TASK NUMBER	
				5f. WORK UNIT NUMBER	
7. PERFORMING ORGANIZATION NAME(S) AND ADDRESS(ES) Korea Atomic Energy Research Institute (KAERI),150 Dukjin dong Yousung gu,Taejon 305-353,Korea (South),KR,305-353				8. PERFORMING ORGANIZATION REPORT NUMBER N/A	
9. SPONSORING/MONITORING AGENCY NAME(S) AND ADDRESS(ES) AOARD, UNIT 45002, APO, AP, 96337-5002				10. SPONSOR/MONITOR'S ACRONYM(S) AOARD	
				11. SPONSOR/MONITOR'S REPORT NUMBER(S) AOARD-044058	
12. DISTRIBUTION/AVAILABILITY STATEMENT Approved for public release; distribution unlimited					
13. SUPPLEMENTARY NOTES					
14. ABSTRACT Successful ultra-fine nano Al2O3 powder was consolidated and sintered using magnetic pulsed compaction. Measurements indicated that many properties in the consolidated Al2O3 bulk have been much improved over the conventional polycrystalline materials. The optimization of the compaction parameters and sintering conditions will lead to the consolidation of Al2O3 nanopowder for the higher density and even further enhanced mechanical properties.					
15. SUBJECT TERMS Powder Compaction, powder manufacturing , Nano-Materials					
16. SECURITY CLASSIFICATION OF:			17. LIMITATION OF ABSTRACT Same as Report (SAR)	18. NUMBER OF PAGES 12	19a. NAME OF RESPONSIBLE PERSON
a. REPORT unclassified	b. ABSTRACT unclassified	c. THIS PAGE unclassified			

nanoalumina powder by magnetic pulsed compaction (MPC) and sintering process, and subsequently characterized them for their microstructure, mechanical properties, and electrical properties. Finally, we are going to apply this result to high power micro-wave window.

2. EXPERIMENTAL PROCEDURE

2-1 Consolidation of Al_2O_3 nanopowder

The starting powder was $\alpha\text{-Al}_2\text{O}_3$ (purity of 99.8%) with an average powder particle size of 50~200 nm. 1.5 grams of raw Al_2O_3 powder was loaded into a die and punch unit whose outer and



Fig. 1 showing the general view of MPC equipment.

inner diameters were 50 and 15 mm, respectively. The Al_2O_3 powder was consolidated with the shape of disc by magnetic pulsed compaction (MPC). Fig. 1 shows the MPC equipment used in this research (pulsed force: up to 1,000KN, compacting pressure: up to 3 GPa, control temperature: up to 500 °C). A graphite paste was used as a lubricant on the die wall and the bottom punch. The pressure of magnetic pulsed compaction (MPC) varied from 0.5 to 2.1 GPa in the room temperature. In order to improve the density and properties, the starting powder was pre-compacted in a die under 110 MPa, 220 MPa, and 330 MPa, respectively and then each precompacted sample was MPCed at room temperature. The MPCed bulks were sintered at 1,450 °C for 3 hrs in an air atmosphere.

2-2 Microstructure and properties of MPCed and sintered bulk

The sintered bodies were used for Vickers hardness test and break down voltage testing after polishing. The MPCed and sintered bulk was polished using diamond paste and thermally etched at a temperature 100 °C. The apparent density of the bulk was measured by the Archimedes method using water and the values averaged. The relative density was calculated assuming a true density of 3.987 g/cm³ for $\alpha\text{-Al}_2\text{O}_3$.

Fracture surface of sintered bulks was observed with a scanning electron microscope (SEM). Grain size analysis was performed on the digitized SEM photographs using image analysis. X-ray diffraction (XRD) patterns were obtained at a scanning rate of 4°/min with 2 θ range from 10 to 80° using a fully automated diffraction with Cu K α (0.15406 nm) radiation. A transmission electron

microscope was utilized to investigate the particle size, shape of the Al_2O_3 powder. Fracture surfaces were examined by scanning electron microscopy (SEM) to investigate fracture model and grain size. Vickers hardness measurements were performed on a Vickers hardness tester using a Vickers indenter with a load of 19.6 N applied for 10 s.

3. RESULTS AND DISCUSSION

3-1. Characteristics of Al_2O_3 nanopowder

Fig. 2(a) shows the typical morphology of the Al_2O_3 nanopowder particles used in this investigation, as observed by FE-SEM. The powders have a size of approximately 50~200 nm, a smooth surface and elliptical shape. Further, several powder particles seem to consist of the large particles appeared to be formed by agglomeration of smaller particles. Fig. 1(b) shows the morphology of Al_2O_3 nano-powder particles observed by TEM. The powder particles have a size range of approximately 100 nm with spherical and elliptical shape. Microstructural investigation at higher magnification reveals that the size of the Al_2O_3 in coarse area varied between 150 and 200 nm.

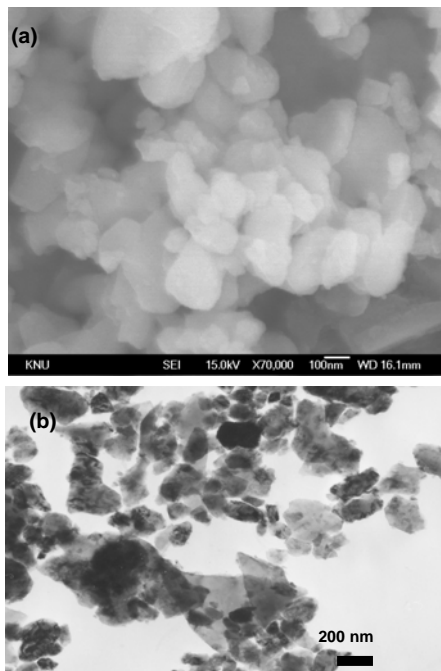


Fig. 2 SEM (a) and TEM (b) morphology of Alumina nanopowder

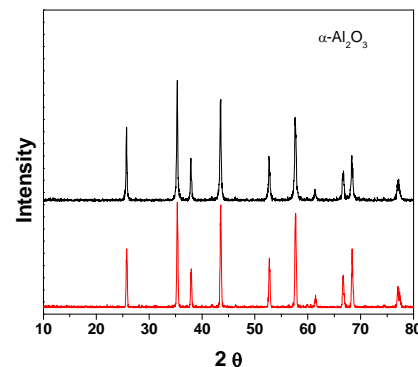


Fig. 3 XRD traces of Alumina nanopowder (a) and bulk (b).

In order to examine the phase information, nanopowder and bulk are analyzed by XRD. Fig. 3 shows X-ray diffraction patterns of Al_2O_3 nanopowder and bulk, respectively. The as-nanopowder consists of the $\alpha\text{-Al}_2\text{O}_3$ phase. In the case of MPCed and sintered bulk, the XRD peaks became shaper and their peak intensities increased. The peak broadening is attributed to crystallite size refinement in the

powder.

3-2. MPC pressure effect on density and properties

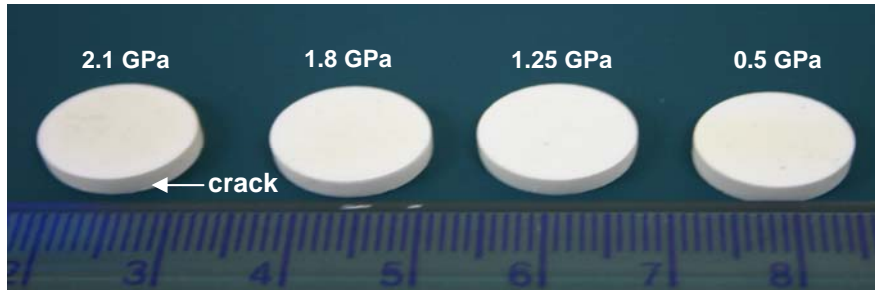


Fig. 4 The appearance of MPCed and sintered bulks as a function of MPC pressure.

For the compaction of Al_2O_3 nanopowders, we are developing a magnetic pulsed method, which is based on converting pulsed electric power to a mechanical pulse and concentrating that pulse in the compaction zone. By using this technique the major challenges can be met which are encountered in the compaction of nanopowders of hard materials, which difficulties arise from the low bulk density and large specific surfaces of these powders. In the present investigation, dynamic

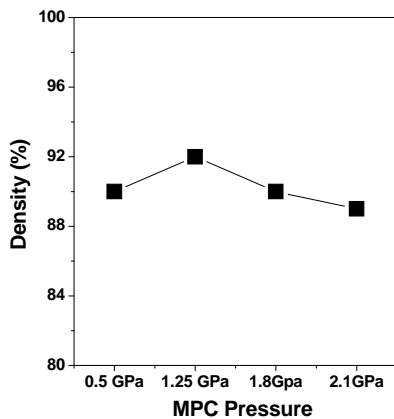


Fig. 5 Variation of density of MPCed and sintered bulk as a function of MPC pressure.

compaction by magnetic pulsed compaction (MPC) is conducted to prepare the Al_2O_3 bulk before sintering. For enhancing the density of MPCed and sintered bulk as a function of MPC pressure (0.5, 1.25, 1.8, and 2.1 GPa) at room temperature has been studied. Fig. 4 shows the morphology of MPCed and sintered Al_2O_3 bulk of a diameter 13 mm and a height of 3.1 mm. The defects such as cracks and dimple on the surface of bulks were not observed. However, the bulks MPCed at 1.8 and 2.1 GPa show cracks on the surface. Especially, the appearance of crack in the MPCed at 2.1 GPa shows more serious result than that of 1.8 GPa.

Fig. 5 shows the density variation of MPCed and sintered ($1450\text{ }^\circ\text{C}$ for 3 h) bulk with MPC pressure. The obtained density of MPCed and sintered bulks is increased with increasing MPC pressure. It was impossible to apply more than 2.1 GPa with MPC due to surface crack of sintered bulk. The highest density of 92 % is achieved in MPCed at 1.25 GPa and sintered bulk. From this result, the maximum pressure required to consolidate the nanopowder without any cracks on the surface of bulk is 1.25 GPa. The bulk compacted at 1.25 GPa reached slightly higher density than the bulk compacted at 0.5 GPa in spite of the same initial density. This may be due to the high packing

density by higher MPC pressure. The consolidation pressure required to consolidate the

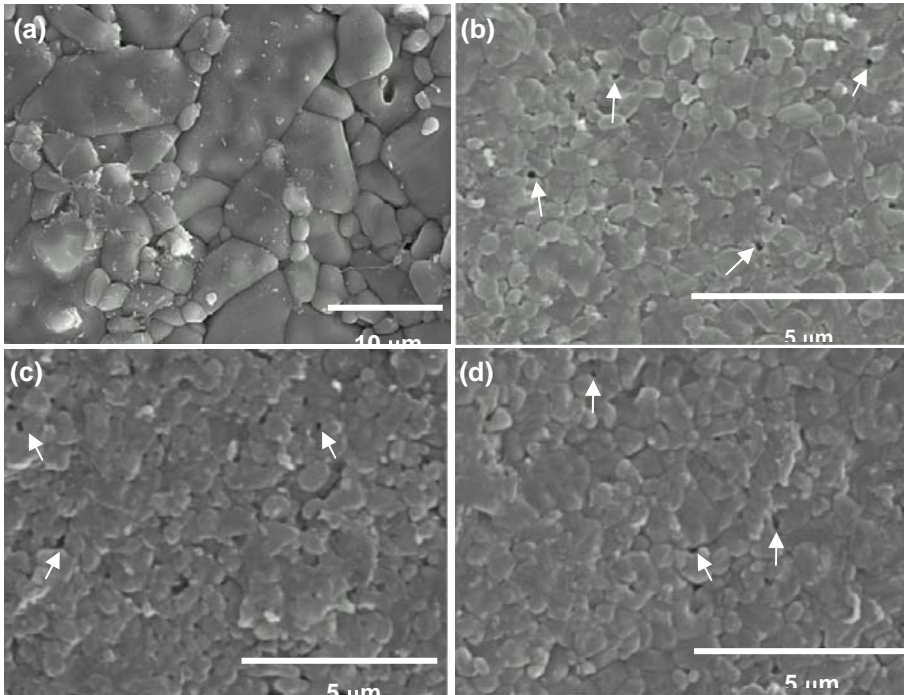


Fig. 6 SEM micrographs of the MPCed and sintered bulks as a function MPC pressure.

nanopowder is related to the force required to push particles together. In order to push two particles together, the applied force must be equal or greater than the resisting force. On pressing at 1.8 GPa, the density is decreased to 90 % due to fine crack on the surface of MPCed and sintered bulk. Further pressing to 2.1 GPa resulted in visible cracking formation on the surface of MPCed and sintered bulk as well as decreasing the density to 89 %. In this

research, the optimum MPC pressure is 1.25 GPa.

Fig. 6 shows the SEM micrographs of the MPCed and sintered bulk as a function of MPC pressure. The resultant microstructure shows the homogeneously distributed Al_2O_3 particle embedded in the

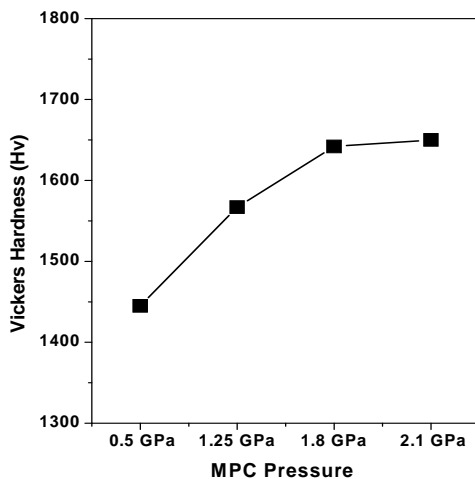


Fig. 7 Vickers hardness of the MPCed and sintered bulks as a function MPC pressure.

Vickers hardness of MPCed and sintered bulk shows different values as a function of MPC pressure. With increasing the MPC pressure, the hardness of bulk was increased. The different

The microstructure of commercial Al_2O_3 plate (Fig. 6 (a)) shows coarse grains and porous among the powder boundaries. Whereas, the microstructure of MPCed and sintered bulk exhibits small grain with fine pores. The features are in the average grain size of $0.66 \mu m$ for the 0.5 GPa and $0.5 \mu m$ for the 2.1 GPa of the MPCed and sintered bulk. On the contrary, the size range of the commercial Al_2O_3 plate is $5.45 \mu m$. FE-SEM analysis thus showed the promise of consolidation of nanopowder with retained ultra-fine microstructures.

Fig. 7 shows the variation of Vickers hardness as a function of the MPC pressure of the MPCed and

Vickers hardness with MPC pressure might be associated with the different density distribution of bulks. In addition, the different size of porosity in different regions can be another important factor leading to different. Despite the porosities, the homogeneously distributed nanoparticles, and small particles spacing in the bulk can be the foundations of the increased hardness.

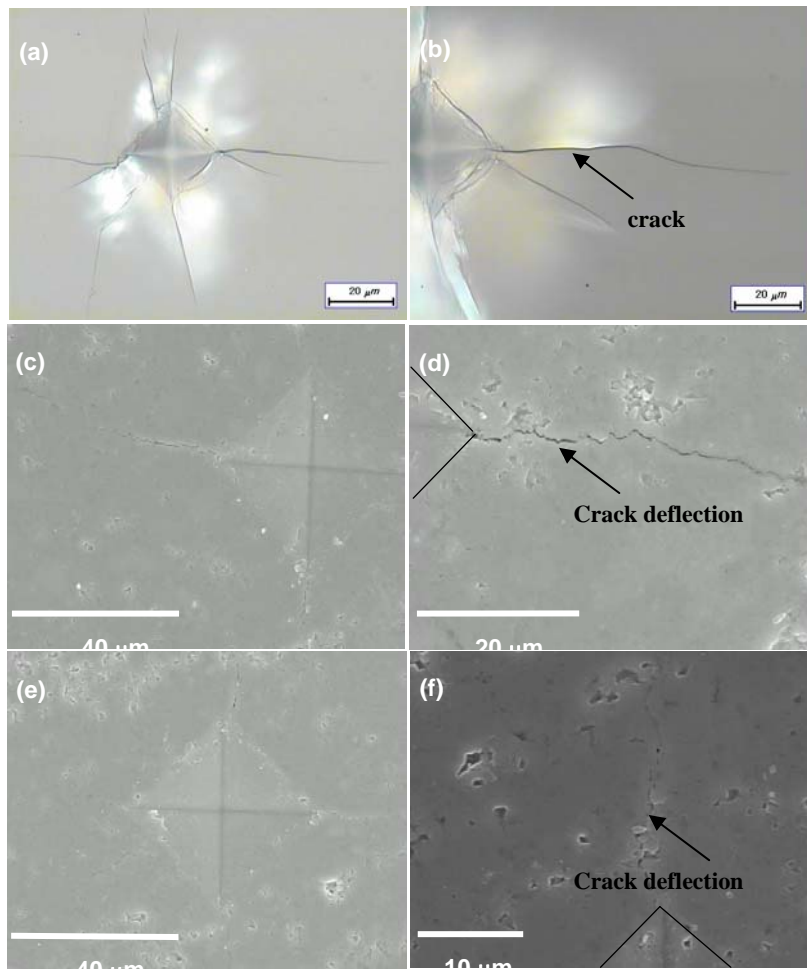


Fig. 8 SEM micrographs of bulks showing cracks formed from the corners of hardness indenters.

The damage and failure of Al_2O_3 bulk is generally associated with initiation and growth of cracks; these can be conveniently observed in fracture surface of specimens, as shown in Fig. 8. Fig. 8 shows representative SEM micrographs of cracks formed from the corner of the indenter. The crack-microstructure interactions which contribute to the fracture toughness are evident in these micrographs. Despite the secondary cracking, the long crack was observed from the indenter of a spire Al_2O_3 as shown in Fig. 8 (a, b). Many cracks formed from each corner of the indenter and propagated easily without

tortuosity. Fig. 8 (c) and (d) show the indenter and cracks formed from the MPCed and sintered bulk with a MPC pressure of 0.5 GPa. Fig. 8 (e) and (f) show the indenter and cracks formed from the MPCed and sintered bulk with a MPC pressure of 1.2 GPa. MPC pressure of 0.5 GPa shows longer crack length than that of 1.2 GPa. In Fig. 8 (e and f) crack deflection was observed as a result of the uniformly dispersed fine particles in the bulk. The interaction between the crack and the fine particles resulted in the crack deflection. Microscopic analysis (Fig. 8 (d) and (f)) demonstrates that the direction of the crack propagation was changed whenever it meets the fine particles in the matrix and propagates around them. Finally, it is expected that the small grains and their homogeneous distribution are more prone to the crack deflection.

It can be observed that the fracture mode of monolithic Al₂O₃ is basically intergranular fracture, and the fracture model changes from intergranular model to transgranular model as MPC pressure is enhanced. Except for the crack deflection toughening, the crack branching and crack bridging are

contributed to the increasement of the fracture toughness and hardness.

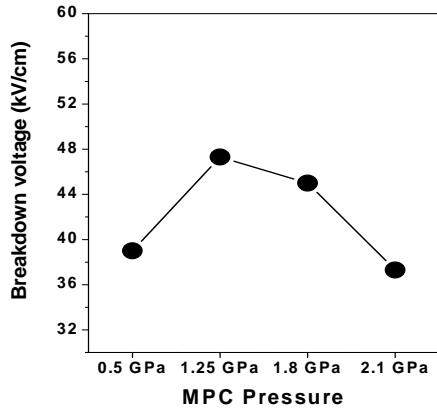


Fig. 9 Variation of breakdown voltage of sintered bulks with MPC pressure.

Fig. 9 shows the break down voltage of MPCed and sintered bulk as a function of MPC pressure. The breakdown voltage of MPCed and sintered bulk increased with increasing MPC pressure from 0.5 GPa to 1.25 GPa. However the value of MPCed and sintered bulk at 1.8 and 2.1 GPa is decreased due to formation of micro and macro cracks on the surface. The maximum breakdown voltage of 47 kV/cm is achieved in MPCed at 1.25 GPa. This result means that the densification of bulk without crack increases the breakdown voltage. Finally, the fracture mechanism of

failure in breakdown voltage testing was also studied as shown in Fig. 10.

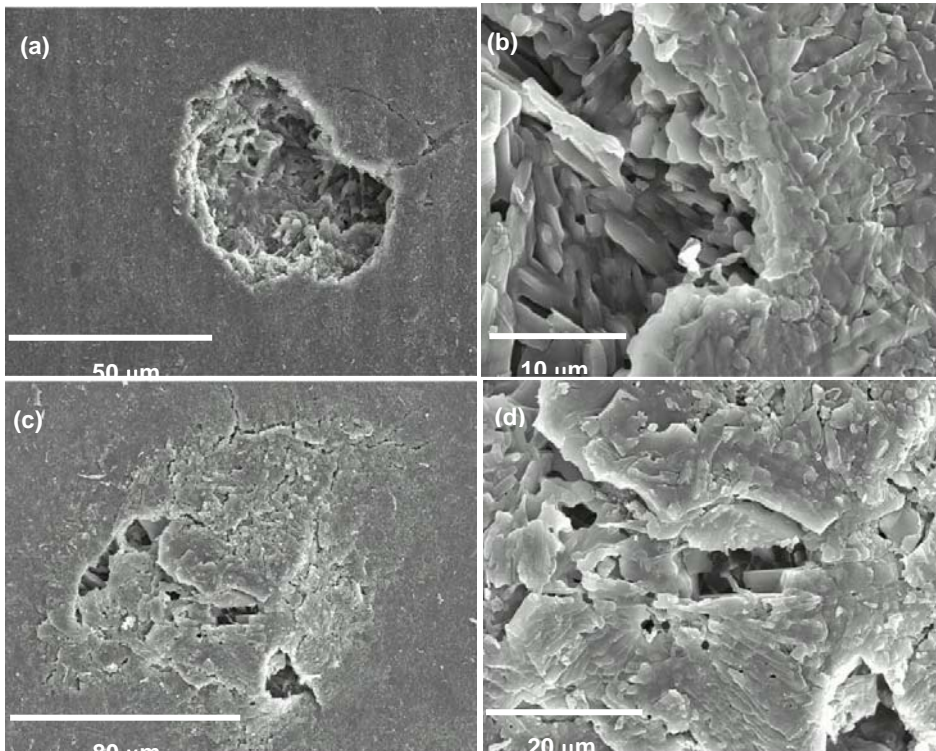


Fig. 10 SEM micrographs of the brackdowned fracture surface of bulks with MPC pressure.

Fig. 10 shows SEM micrographs of the breakdowned fracture surface of the bulks. The figure shows the fully formed hole (Fig. 10 (a)) and the partially formed (Fig. 10 (c)), retained cracks as shown in Fig. 10 (d). The specimen of 0.5 GPa (Fig. 10 a and b) shows a deep hole formed during breakdown voltage testing. However, the fracture surface

observed was basically different in the specimen of 1.2 GPa (Fig. 10 c and d). Fracture analysis demonstrates that low density is more

prone to failure than the higher one; the lower the density the greater is the probability to have cracks and hole in it and consequently the lower the load it can withstand before fracture. Further, since the alloy with the higher bulk is stronger, cracks in the stronger bulk forms shallow hole.

3-3. Pre-compaction effect on density and properties

In order to improve the density and properties, the starting powder was pre-compacted in a die under 110 MPa, 220 MPa, and 330 MPa, respectively and then each pre-compacted sample was MPCed at room temperature. Finally, the MPCed bulks were sintered at 1,450 °C for 3 h in an air. Fig. 11 shows the morphology of pre-compacted, MPCed, and sintered Al_2O_3 bulk as a function of pre-compaction pressure. The defects such as cracks and dimple on the surface of samples were not observed. To evaluate the effects of the different pre-compaction conditions, the author used the density of the sample as a measure of compaction efficiency.

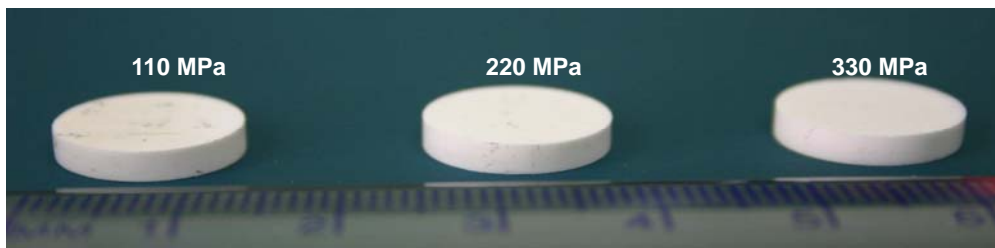


Fig. 11 The appearance of pre-compacted, MPCed and sintered bulks with pre-compaction pressure.

from plot that the density increases with increasing pre-compaction pressure from 0 MPa to 220 MPa and then saturated at 94 % on pre-compaction pressure beyond 330 MPa. The highest density of 94 % is achieved in the pre-compacted sample at 220 MPa, while the density of the sample compacted without pre-compaction is 92 %. It means that pre-compaction of powder before MPC improves the final density of sintered bulk. Because these powders are not expected to deform plastically during compaction like metals, the reported increase in hardness would be expected to be a result of tighter and more efficient packing density.

Fig. 13 shows the SEM micrographs of the pre-compacted, MPCed, and sintered bulk as a function of the pre-compaction pressure. The authors estimated an average grain size using the line intercept method. The relative density of the 110 MPa sample was 93 % and most of the resolved porosity appeared to be isolated at grain

Fig. 12 shows the density variation of pre-compacted, MPCed and sintered bulks as a function of pre-compaction

pressure. It is clear

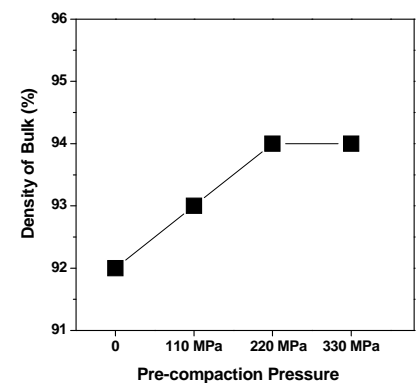


Fig. 12 Density of MPCed and sintered bulks with pre-compaction pressure.

interstices. The authors noticed that, as the pre-compaction pressure increased, the average grain size decreased and resulting microstructure was more homogeneous after sintering. Evidence of these observation was also seen in the sample pre-compacted at 330 GPa. In a similar analysis of pre-compacted sample at 330 GPa, the average grain size was determined to be 0.49 μm and the relative density was also 94 %. The pores in these samples were exclusively accommodated at grain interstices.

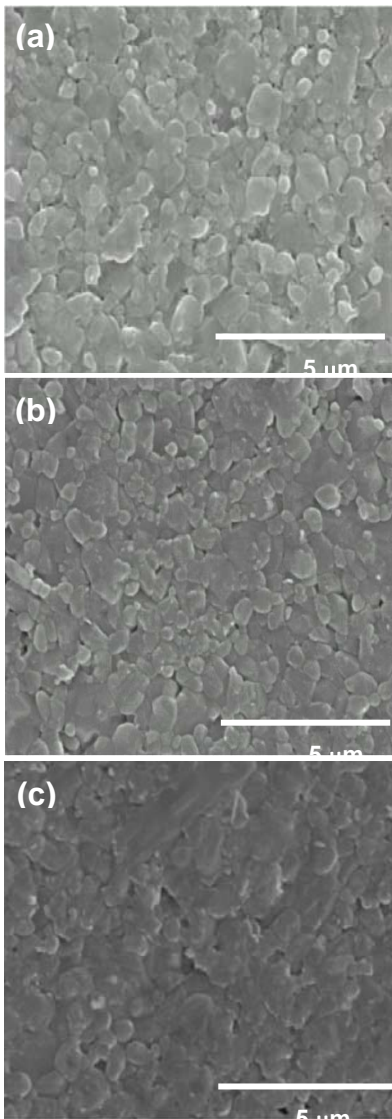


Fig. 13 SEM micrographs of the pre-compacted, MPCed and sintered bulks as a function of pre-compaction pressure.

performed on the pre-compacted, MPCed, and sintered samples, and the results are shown in Fig. 15. Under the same load, indentation marks in the consolidated bulk with pre-compaction are smaller than those in the samples without pre-compaction because the sample with pre-compaction

Vickers hardness also presented as a function of pre-compaction pressure of bulks as show in Fig. 14. With increasing pre-compaction pressure, the hardness of bulk is increased. This suggests that particle rearrangement during pre-compaction is occurring at lower pressures. The improved hardness with increasing pre-compaction pressure might be associated with the improved density of bulk. These results clearly indicate that pre-compaction for MPC and sintering is an efficient process to improve the density and Vickers hardness. In addition the structural characteristics which are controlled by the consolidation and processing, such as porosities, internal stress, etc., may play

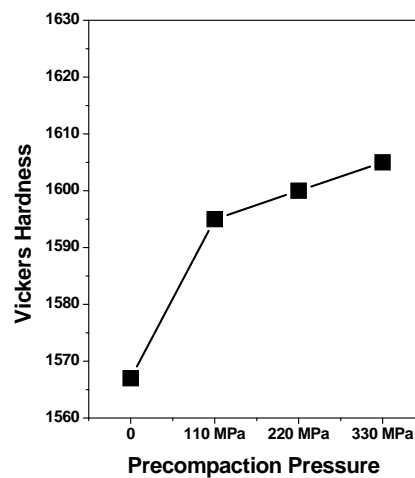


Fig. 14 Vickers hardness of the MPCed and sintered bulks as a function of pre-compaction pressure

an important role in the properties. It is ambiguous to distinguish the contribution to the property enhancement from the grain size effect or from other effects such as pores or strain with the consolidated samples.

The indentation fracture method is often employed to characterize the relative fracture toughness and hardness of materials. An indentation

fracture examination was

has a higher hardness. Under a load of 19.6 N, many large cracks caused by an indentation were observed in the MPCed and sintered bulk without pre-compaction, whereas few small cracks were

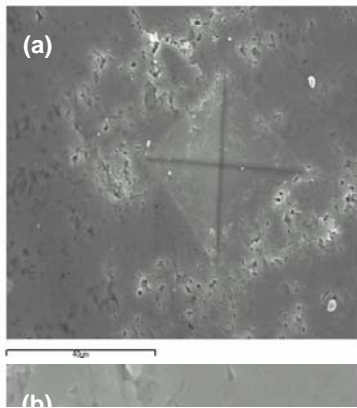
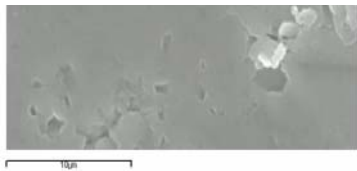


Fig. 15 SEM micrographs of bulks showing cracks formed from the corners of hardness indenters.



presented in the MPCed and sintered bulk with pre-compaction. This result suggests that the sintered Al_2O_3 bulk with pre-compaction possess higher apparent fracture toughness relative to that of the sample without pre-compaction.

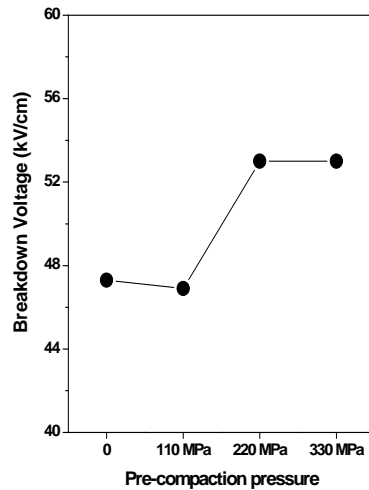


Fig. 16 Variation of breakdown voltage of sintered bulks with pre-compaction pressure.

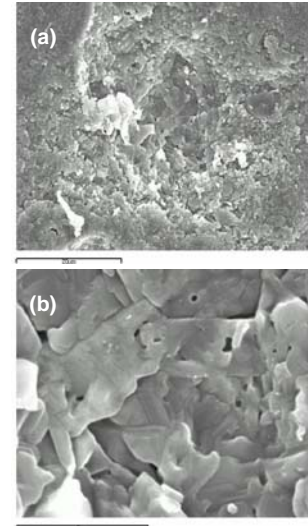


Fig. 17 SEM micrographs of the breakdowned fracture surface of bulks with pre-compaction pressure.

Fig. 16 shows the breakdown voltage of MPCed and sintered bulk as a function of pre-compaction pressure. The breakdown voltage of sintered bulks increased with increasing pre-compaction pressure. The highest breakdown voltage of 53 kV/cm is achieved in pre-compacted specimens at 220 MPa and 330 MPa. Fig. 17 shows SEM micrographs of the breakdowned fracture surface of the pre-compacted bulk at 220 MPa. The micrograph shows the very shallow hole. The formed hole in bulk was smaller than that of the bulks without pre-compaction due to the high density. Fig. 17 (b) shows the high magnification micrograph from the fracture surface. The microstructure shows the coarse microstructure due to the high temperature during voltage loading. However, it was difficult to observe the sever cracks which were easily observed in the samples without pre-compaction. The density and properties of MPCed and sintered bulks with experimental conditions are summarized in Table 1.

Table 1 Density and room-temperature properties of MPCed and sintered bulk with experimental conditions.

Experimental conditions	Bulk condition	Density (%)	Average Vickers hardness	Breakdown Voltage (kV/cm)
Commercial Al₂O₃ plate	Good	.	1500	35.47
Uniaxial static compaction (110 MPa) + Sintering (1,450 °C for 3 h)	Good	90	1,400	39.9
MPC (0.5 GPa) + Sintering (1,450 °C for 3 h)	Good	90	1,445	39.01
MPC (1.25 GPa) + Sintering (1,450 °C for 3 h)	Good	92	1567	47.28
MPC (1.8 GPa) + Sintering (1,450 °C for 3 h)	Fine crack	90	1,642	45.03
MPC (2.1 GPa) + Sintering (1,450 °C for 3 h)	Coarse crack	89	1,650	37.25
Pre-compaction (110 MPa) + MPC (1.25 GPa) + Sintering (1,450 °C for 3 h)	Good	93	1,590	46.84
Pre-compaction (220 MPa) + MPC (1.25 GPa) + Sintering (1,450 °C for 3 h)	Good	94	1,591	52.67
Pre-compaction (330 MPa) + MPC (1.25 GPa) + Sintering (1,450 °C for 3 h)	Good	94	1,603	53.06

Conclusions

Herein, we reported for the first time, the successful consolidation of Al₂O₃ powder with retained ultra-fine structure using MPC and sintering. Measurements in the consolidated Al₂O₃ bulk indicated that many properties have been much improved relative to the conventional polycrystalline materials. The homogeneously distributed fine microstructure and high density in the MPCed and sintered bulk showed relatively higher hardness and breakdown voltage than the other samples. The magnetic pulsed compaction method permits making compacts of Al₂O₃ nanopowders with densities up to 94 %, whereas the density of stationary compaction is 90 %. A further increase in the density of specimens compacted by the magnetic pulsed compaction is not only determined by the amplitude of the pushing pressure but also other important process parameters, such as density prior to compaction and sintering temperature.

The highest density and breakdown voltage in this research is 94 % and 53 kV/cm, respectively. The higher hardness, fracture toughness, and breakdown voltage could be attributed to the crack deflection by a homogeneous distribution and the retention of nanostructure, regardless of the presence of porosities.

Finally, optimization of the compaction parameters and sintering conditions will lead to the consolidation of Al₂O₃ nanopowder with higher density and even further enhanced mechanical properties.

REFERENCES

1. C. H. Shek, J. K. L. Lai, T. S. Gu, and M. Lim, *Nanostruct. Mater.* **8 (5)**, 605-610 (1997).
2. R. A. Andrievski, *J. Mater. Sci.* **29**, 614 (1994).
3. S. C. Wang and W. C. J. Wei, *Nanostruct. Mater.* **10(6)**, 983-1000 (1998).
4. J. Freim, J. Mckittrick, J. Katz, and K. Sickafus, *Nanostruct. Mater.* **4**, 371 (1994).
5. S. L. Wu, L. C. Dejonghe, and M. N., Rahaman, *J. of the Ameri. Ceramic. Soci.* **79**, 2989 (1996).
6. G. H. Lee, C. K. Rhee, M. K. Lee, W. W. Kim, and V. V. Inanov, *Mater. Sci. Eng.* **A375-377**, 604-608 (2004).
7. S. J. Hong, G. H. Lee, C. K. Rhee, and G. S. Lee, *Maer. Sci. Eng.* (2005) in press.